Clays and Clay Minerals, Vol. 44, No. 1, 96–112, 1996.

DIAGENESIS AND METAMORPHISM OF CLAY MINERALS IN THE HELVETIC ALPS OF EASTERN SWITZERLAND

HEJING WANG,[1,2] MARTIN FREY,[1] AND WILLEM B. STERN[1]

[1] Mineralogisch-Petrographisches Institut der Universität, Bernoullistrasse 30, CH-4056 Basel, Switzerland

[2] Present address: Department of Geology, Peking University, Beijing 100871, P.R. China

Abstract—Helvetic sediments from the northern margin of the Alps in eastern Switzerland were studied by clay mineralogical methods. Based on illite "crystallinity" (Kübler index), the study area is divided into diagenetic zone, anchizone and epizone. Data on the regional distribution of the following index minerals are presented: smectite, kaolinite/smectite mixed-layer phase, kaolinite, pyrophyllite, paragonite, chloritoid, glauconite and stilpnomelane. Isograds for kaolinite/pyrophyllite and glauconite/stilpnomelane are consistent with illite "crystallinity" zones. Using the ordering of mixed-layer illite/smectite, the diagenetic zone is subdivided into three zones. The illite domain size distribution was analyzed using the Warren-Averbach technique. The average illite domain size does not change much within the diagenetic zone, but shows a large increase within the anchizone and epizone. The average illite b_o value indicates conditions of an intermediate-pressure facies series.

The Helvetic nappes show a general increase in diagenetic/metamorphic grade from north to south, and within the Helvetic nappe pile, grade increases from tectonically higher to lower units. However, a discontinuous inverse diagenetic/metamorphic zonation was observed along the Glarus thrust, indicating 5–10 km of offset after metamorphism. In the study area, incipient metamorphism was a late syn- to post-nappe-forming event.

Key Words—Clay mineralogy, Diagenesis, Helvetic Alps, Incipient metamorphism, Switzerland.

INTRODUCTION

Diagenetic and very low-grade metamorphic sediments are widespread in external parts of the Alps (Frey 1986). Therefore, an understanding of incipient metamorphism is important to unravel the tectonothermal evolution of such areas. Contrasting methods have been applied to quantify the degree of incipient metamorphism during Alpine orogenesis such as illite "crystallinity," index minerals, coal rank and fluid inclusion data. The aim of this study is to provide new information on diagenesis and incipient metamorphism of the Helvetic Alps of eastern Switzerland based on clay mineral data. Besides the classical approach using illite "crystallinity" and index minerals, additional information was obtained from the ordering of illite/smectite mixed-layer minerals and the domain size of illite. Information on coal rank, based on vitrinite reflectance data using the same samples of the present study, is given by Erdelbrock (1994).

GEOLOGICAL SETTING

The study area is located in northeast Switzerland and extends from Appenzell in the north to Chur in the south (45 km) and from Lake Walen in the west to the Rhine River in the east (30 km) (Figure 1). Tectonically the study area belongs to the Helvetic zone along the northern margin of the Alps. To the north, nappes of the Helvetic zone override the Tertiary clastics of the adjoining Molasse basin, a foredeep which formed during the later stages of the Alpine collision. To the south and east, the Helvetic nappes are overlain by the Penninic nappe system. The Mesozoic sediments making up the largest part of the Helvetic zone comprise essentially a carbonate shelf sequence of the northern European margin. In the course of the Alpine collision the Penninic nappes were thrust onto the Helvetic zone. During this process, the rocks of the Helvetic zone were buried, deformed and metamorphosed up to lower greenschist facies conditions.

The Helvetic zone of the area investigated is subdivided by the Glarus thrust, which has a displacement of up to 40 km, into the Helvetic nappes (above) and the Infrahelvetic complex (below). The Helvetic nappes represent classic detachment tectonics, whereas the Infrahelvetic complex is a thick-skinned fold-and-thrust belt, cored by the Aar massif basement uplift. The stratigraphic sequence of the Helvetic zone includes Permian conglomerates, Triassic dolomites, various thick limestones of Jurassic and Cretaceous age and Tertiary sandstones that are interbedded with various shaly and marly horizons. On top of the Helvetic Säntis nappe, Southhelvetic units and separated by the basal Penninic thrust, several Penninic klippes are found (Figure 1). The Southhelvetic units comprise mainly limestones and marls of Upper Cretaceous to Eocene age. The Penninic klippes consist mainly of Cretaceous Northpenninic flysch. For more detailed information on the geologic evolution of the Helvetic zone, the reader is referred to Trümpy (1980), Pfiffner (1986) and Pfiffner et al. (1990).

Very low-grade metamorphism of the Helvetic zone of eastern Switzerland has been studied by many au-

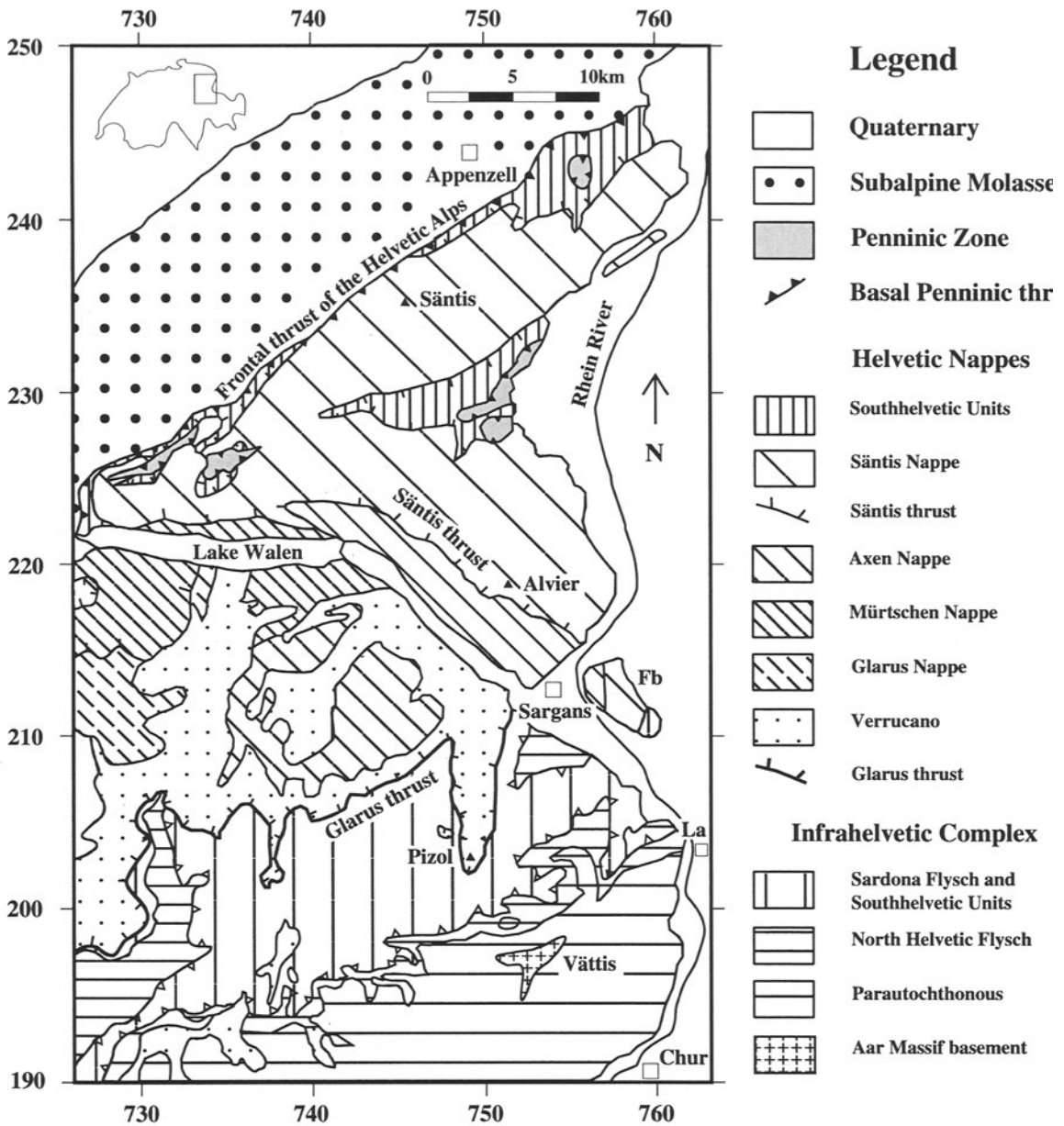

Figure 1. Tectonic map of NE Switzerland, modified after Spicher (1980). Marginal numbers refer to the Swiss coordinate network system. Fb = Fläscherberg, La = Landquart.

thors, using mainly the illite "crystallinity" technique and index minerals, supplemented by a few virtrinite reflectance and fluid inclusion data. Frey (1970) noted a general increase of illite "crystallinity" from the lower anchizone south of Lake Walen to the epizone in the parautochthonous cover of the Aar massif. Frey (1988) found epizonal illite "crystallinities" in the Verrucano of the lower Helvetic nappes and mid-anchizonal values in the underlying flysch units of the Infrahelvetic complex. The discontinuous inverse metamorphic zonation was explained by post-metamorphic thrusting along the Glarus thrust. Frey et al. (1973) and Frey (1987a) mapped index minerals in glauconite-bearing limestones. A stilpnomelane-in isograd was located in the mid-anchizone and a biotite-in isograd at the beginning of the epizone. Frey (1987b) located the isograd kaolinite + quartz = pyrophyllite + H_2O, running in a WSW-ENE direction close to the eastern end of Lake Walen, and estimated metamorphic conditions at the isograd from vitrinite reflectance and fluid inclusion data to be 1.3–2.1 kbar and 240–270°C at a water activity of 0.6–0.8. Recent-

https://doi.org/10.1346/CCMN.1996.0440109 Published online by Cambridge University Press

ly, Erdelbrock et al. (1993) presented a coalification map of the study area, based on about 450 vitrinite reflectance values. The thermal maturity was found to increase from ca. 0.5% R_r in the Subalpine Molasse in the north to R_{max} >5% in the south. Hunziker et al. (1986) dated the main phase of Alpine metamorphism at 30–35 Ma, based on concordant K-Ar, $^{40}Ar/^{39}Ar$ and Rb-Sr illite ages, while a second age group between 20 and 25 Ma was attributed to movements along the Glarus thrust.

METHODS

MATERIAL STUDIED. Some 386 samples were analyzed. Lithologies included ~40% shales and slates, ~30% sandstones, ~20% marls and ~10% limestones and marbles. The location of the samples is given in Figure 2. Note the uneven sample density with few samples west of Sargans and in the southernmost part of the study area.

SAMPLE PREPARATION. Samples were cleaned with a steel brush, crushed into small pieces with a hammer and ~70 g of sample were ground in a tungsten-carbide swing-mill for 30 sec. Carbonate was removed by treating with 5% acetic acid and by washing with deionized water. The <2 μm fraction was prepared using differential settling tubes and millipore filters with 0.1 mm pore size. The clay fraction was then Ca-saturated with 2N $CaCl_2$. Oriented slides were prepared by pipetting suspensions onto glass slides (~5 mg/cm²) and allowing it to air-dry. Glycolated mounts (for 228 samples) were prepared in a glycol steam bath at 60°C overnight. Heat-treated mounts (for 48 samples) were prepared in an oven at 375 or 500°C for 1 h. Randomly oriented samples were prepared using the technique proposed by Handschin and Stern (1989) and Stern (1991) needing only 20 mg of material.

X-RAY DIFFRACTION (XRD). Measurements were performed with a Siemens D500 diffractometer, optimized for counting statistics and acceptable resolution (Table 1).

DOMAIN SIZE ANALYSIS. The method proposed by Warren and Averbach (1950) and the Scherrer equation were used to investigate the domain size or the mean domain thickness. Analyses were performed on XRD patterns after deconvolution. For the Scherrer equation, the constant K was set at 1.84 for layer-minerals according to Klug and Alexander (1974, p. 667).

GUINIER CAMERA X-RAY ANALYSIS. The <2 μm fractions of 41 samples were analyzed using a Guinier-de Wolff camera for the "060" d-spacing analysis. Measuring conditions were with $FeK\alpha_1$ radiation at 36 kV, 20 mA and with 16 h. exposure time. The films were transformed into diffractograms by use of a CR-650S densitometer.

RESULTS AND DISCUSSION

Incipient metamorphism in the study area will be documented by use of several index minerals and various properties of illite, mixed-layer illite/smectite and chlorite. Results from illite "crystallinity" will be presented first, because it will serve as a reference frame for other indicators of incipient metamorphism.

Illite "Crystallinity"

GENERAL. Illite "crystallinity" (IC) was measured from X-ray diffractograms of air-dried preparates using the technique of Kübler (1967, 1968). This IC index is defined as the full width at half maximum intensity (FWHM) of the first illite basal reflection at around 10 Å, expressed as a difference in 2Θ values. The numerical value of the Kübler index decreases with improving "crystallinity." Since illite/smectite mixed-layer minerals are abundant in the study area, especially in the diagenetic zone (see below), the measurement of the FWHM includes both illite and illite/smectite basal reflections. For simplicity, however, the term IC will be retained here.

RESULTS. IC was determined on 368 samples. In order to avoid interfering basal reflections, paragonite- and pyrophyllite bearing samples from the anchizone were avoided, but some paragonite-bearing samples showing epizonal IC values were retained. FWHM values range from 2.50 to 0.16 °Δ2Θ. The regional distribution of IC data is depicted in Figure 2, grouping the data into four classes using an arbitrarily chosen value of 0.80 °Δ2Θ and the limiting IC values of 0.42 and 0.25 °Δ2Θ for the anchizone. In general, IC improves southward. The transition from the diagenetic zone to the anchizone is shown as a 2–3 km broad band limited by two lines labelled 1 and 1′. Line 1 is defined by the first anchizonal IC values going southward (neglecting three anchizonal values east of Appenzell), and line 1′ is defined by the disappearance of diagenetic IC values (neglecting four data points south of Sargans). In a similar way, the transition from the anchizone to the epizone is shown as a 2–3 km broad band limited by two lines labelled 2 and 2′. Line 2 is defined by the first epizonal IC values going southward (neglecting four epizonal data points further north, three from the Verrucano and one from the basal part of the Axen nappe), and line 2′ is defined by the disappearance of anchizonal IC values.

The following tectonic units belong to the diagenetic zone (compare Figures 1 and 2): the Subalpine Molasse, Penninic and Southhelvetic units as well as the major part of the underlying Helvetic Säntis nappe (excluding a small area east of Alvier and the Fläscherberg east of Sargans). Localities with IC values >0.8 and 0.8–0.43 °Δ2Θ are intermixed in the diagenetic zone. The transition from the diagenetic zone to the anchizone occurs mainly in the lower part of the

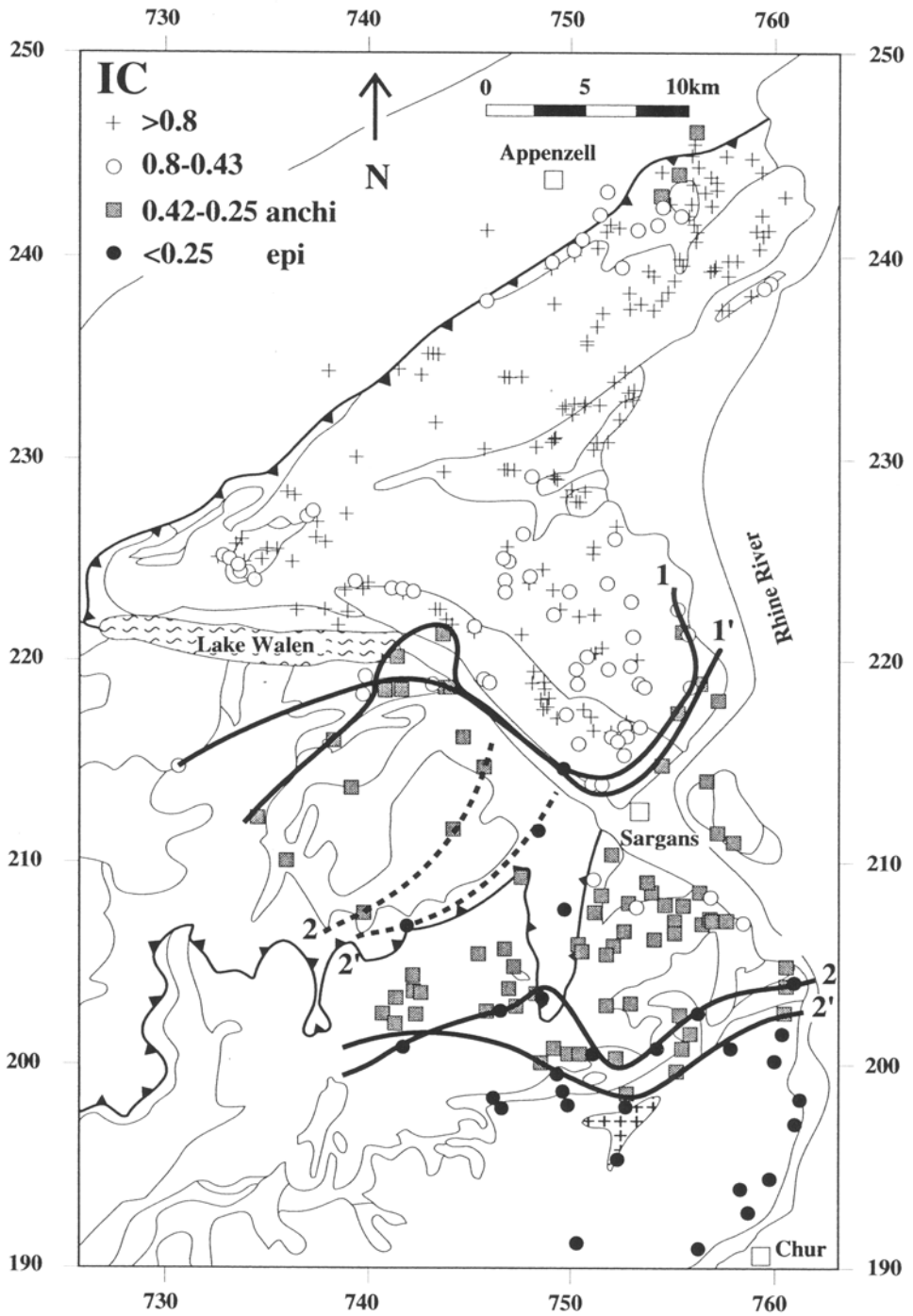

Figure 2. Illite "crystallinity" distribution map. Lines 1 and 1′ indicate the transition from the diagenetic zone to the anchizone. Lines 2 and 2′ indicate the transition from the anchizone to the epizone. The two dashed lines 2 and 2′ W of Sargans indicate the transition from the anchizone to the epizone in the Verrucano.

Axen nappe northeast of the Seez Valley (between Lake Walen and Sargans). This area is characterized by a strong relief of almost 2 km. Further to the west, this boundary is located in the Mürtschen nappe southeast of Lake Walen. North-northeast of Sargans, this boundary is cutting through the Säntis thrust, separating Säntis and Axen nappes. The following tectonic units of the study area belong to the anchizone: the Axen nappe and the Verrucano southeast of the Seez Valley (Flumserberge), Axen and Säntis nappe of the

https://doi.org/10.1346/CCMN.1996.0440109 Published online by Cambridge University Press

Table 1. Instrumental conditions and measurement procedure.

Equipment	Diffractometer SIEMENS D-500			
Radiation	Cu, 40kV, 30mA, no primary filter			
Slits	automatic divergence set at 3°, slits on primary side 3°; secondary side 1°, 0.05 and 0.15 mm. Graphite monochromator			
Goniometer	routine measurement			cell parameter
	low angle	medium angle	high angle	low to high angle
	2-15°2Θ	15-42°2Θ	42-48°2Θ	5-65°2Θ
	0.05° increment	0.02°	0.02°	0.02°
	30 sec.	1 sec.	10 sec.	10 sec.
Computer	Sicomp 32-20 80-386 with internal and external hard discs and CD-rom for JCPDS-data			
Software	Diffrac AT Version 3.2 by Socabim/Siemens 1986, 1993, JCPDS data bank system version 2.14. Sets 1-43, PDF-1, 2			
$K\alpha_2$	not stripped			
IC (Kübler index)	measured from the unresolved 10 Å complex using single peak-option in Diffrac AT			
$d_{001/001}$ of I/S	deconvoluted from the 10 Å complex for glycolated samples			
Domain size	I/S and illite were deconvoluted using Pearson function for the 10 Å complex at air-dried state, the backgrounds were subtracted, no smoothing operation. The deconvoluted profiles were then transferred to the WIN-CRYSIZE programme (version 1.03, Sigma-C. 1991–1994), from which the average domain size of I/S and illite, and the domain size distributions were calculated using the W-A method. Single crystal of muscovite was used as standard			
b_o	The background was subtracted first, no smoothing operation, zoom editing technique was used. At least 20 reflections of illite were edited and transferred to the WIN-METRIC programme (version 2.0B, Sigma-C. 1991–1994), from which the cell parameters were refined using the least square method assuming a $2M_1$ polytype for all investigated samples. The tolerances are 0.08–0.05°2Θ; rejected reflections less than 10%			

Fläscherberg, and major parts of the Sardona flysch, South Helvetic units and North Helvetic flysch. The transition from the anchizone to the epizone is located mainly in the North Helvetic flysch west of Landquart, but further to the west this transition takes place in the Sardona flysch. Epizonal conditions are encountered in the parautochthonous of the Aar massif, but also in the Verrucano north of Pizol above the Glarus thrust.

DISCUSSION. IC is dependent on many variables, including temperature, fluid chemistry and pressure, stress, duration of alteration, illite chemistry, interfering basal reflections of other phases and experimental conditions (Frey 1987a; Yang and Hesse 1991). Following Kübler (1967, 1968) it is believed that temperature is the most important variable affecting IC in the study area, because the lower and higher anchizone boundaries are subparallel to isorank lines determined by vitrinite reflectance (Erdelbrock 1994).

The following conclusions can be drawn from the IC distribution pattern of Figure 2: 1) Penninic klippes in the northern part of the study area seem to have reached a similar stage of diagenesis as the underlying Southhelvetic units and the Säntis nappe; 2) The lower and higher anchizone boundaries cut through important thrust planes. Therefore, incipient metamorphism occurred after these tectonic movements; and 3) Epizonal conditions were reached in the Verrucano northwest of Pizol above the Glarus thrust but anchizonal conditions exist in the flysch units below the Glarus thrust. This discontinuous inverse metamorphic zonation is explained by post-metamorphic thrusting along the Glarus thrust. The same phenomenon was already observed for an identical tectonic situation 20 km further to the west (Frey 1988). The amount of this post-metamorphic thrusting can be estimated as 5–10 km, corresponding to the distance between the anchizone-epizone boundary in the Verrucano west of Sargans (dashed lines in Figure 2) and the same boundary in the Infrahelvetic complex. Using vitrinite reflectance data, Erdelbrock (1994) deduced an amount of 5.5 km.

Chlorite "Crystallinity"

GENERAL. Chlorite 7 Å peak width measured under the same experimental conditions as illite 10 Å peak width is used to determine chlorite "crystallinity" (CC). Arkai (1991) proposed that CC "can be applied as a reliable regional, statistical technique complementary with, or instead of, the illite crystallinity method."

RESULTS AND DISCUSSION. Figure 3 shows that chlorite has an enhanced "crystallinity" compared to that of illite from the same sample. Due to the rather poor correlation between IC and CC, the latter was not used as an indicator of incipient metamorphism in this study.

https://doi.org/10.1346/CCMN.1996.0440109 Published online by Cambridge University Press

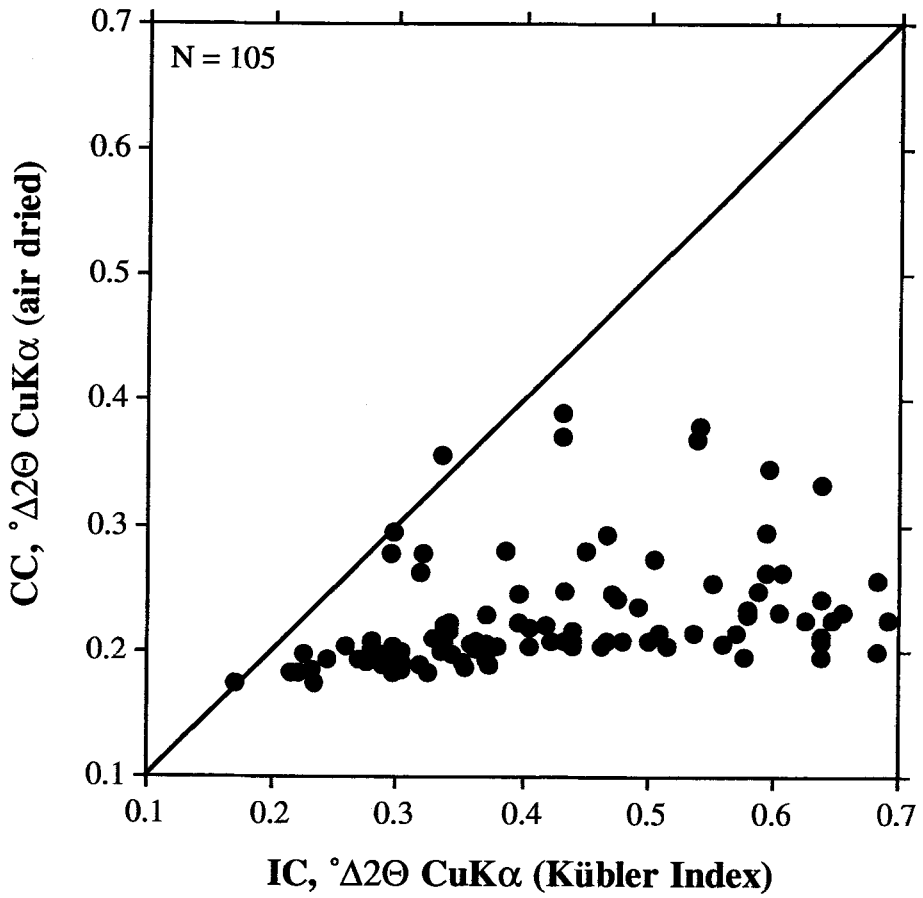

Figure 3. Illite "crystallinity" vs chlorite "crystallinity." The line of equal IC and CC values is indicated for visual inspection.

Regional Distribution of Index Minerals

SMECTITE. Smectite was identified by the strong 001 reflection at about 15 Å on air-dried preparates, shifting to about 17 Å after glycolation, and the 002 reflection at about 8.45 Å. After heating at 500°C for 1 h. these smectite reflections disappeared and the intensity of the first illite basal reflection increased. The position of the (060) reflection at 1.499 Å is indicative for dioctahedral smectite. Pure smectite was only found in 3 sandstones and 4 pelitic samples of the Subalpine Molasse near Appenzell (Figure 4), indicating temperatures <100°C (Velde 1985, p. 115).

KAOLINITE/SMECTITE MIXED-LAYER PHASE. (K/S) was identified by its characteristic peaks and shoulders at spacings of 7.43–7.70 Å and 3.48–3.53 Å after glycolation and by the shift of these peaks after heat treatment at 375°C (Figure 5). In addition, a slightly elevated background was observed between 13–15° 2Θ on glycolated and heat-treated XRD traces. From comparison with calculated diffractograms for the K/S compositional series (Moore and Reynolds 1989, Table 7.5), our K/S are randomly interstratified and contain about 75%–90% kaolinite layers. K/S was detected in four pelitic samples from the Upper Cretaceous (Amden shales) and the Lower Tertiary (Globigerina shales) belonging to the Säntis nappe and Southhelvetic units near the Alpine border (Figure 4).

KAOLINITE. (Kln) was distinguished from chlorite by resolved reflections at about 25° 2Θ CuKα. For kaolinite-poor samples containing large amounts of chlorite, an acid treatment with HCl was used. A few kaolinite occurrences from the study area were already reported by Briegel (1972) and Burger (1982), and Frey (1987b) documented two localities containing kaolinite + pyrophyllite in the same sample. In the course of this study, 29 new kaolinite occurrences were found (Figure 6) mainly in pelites, marls and sandstones of the Subalpine Molasse, Penninic and South Helvetic units and the Säntis nappe. With one exception, all kaolinite localities belong to the diagenetic zone (compare with Figure 2), while the Kln + Prl locality at the eastern end of Lake Walen is from the transition to the anchizone.

https://doi.org/10.1346/CCMN.1996.0440109 Published online by Cambridge University Press

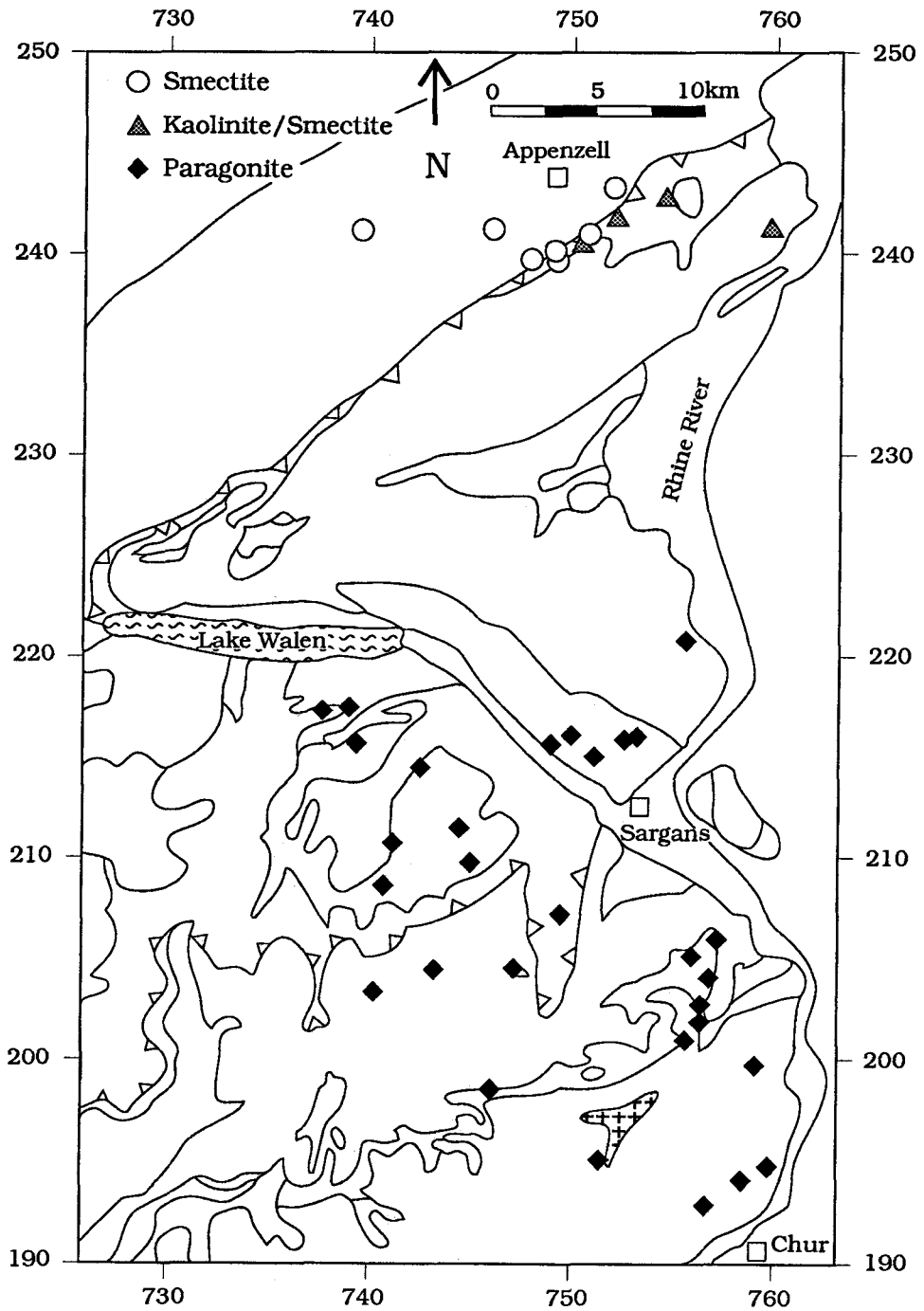

Figure 4. Distribution map for smectite, mixed-layer kaolinite/smectite and paragonite.

PYROPHYLLITE. (Prl) was easily identified by its first three basal reflections. Most of the pyrophyllite occurrences shown in Figure 6 were already documented by Frey (1987b). Three new occurrences of pyrophyllite were added in this study, two from Upper Liassic black shales and one from a Middle Jurassic (Mols fm.) pelitic sandstone, all located closely together in the lower Axen nappe between Sargans and Lake Walen. These new findings allow for a more precise location of the isograd Kln + Qtz = Prl + H_2O in the study area, running from the eastern end of Lake Walen in an almost west-east direction and crossing the Säntis thrust. In terms of IC data, this isograd is located approximately at

https://doi.org/10.1346/CCMN.1996.0440109 Published online by Cambridge University Press

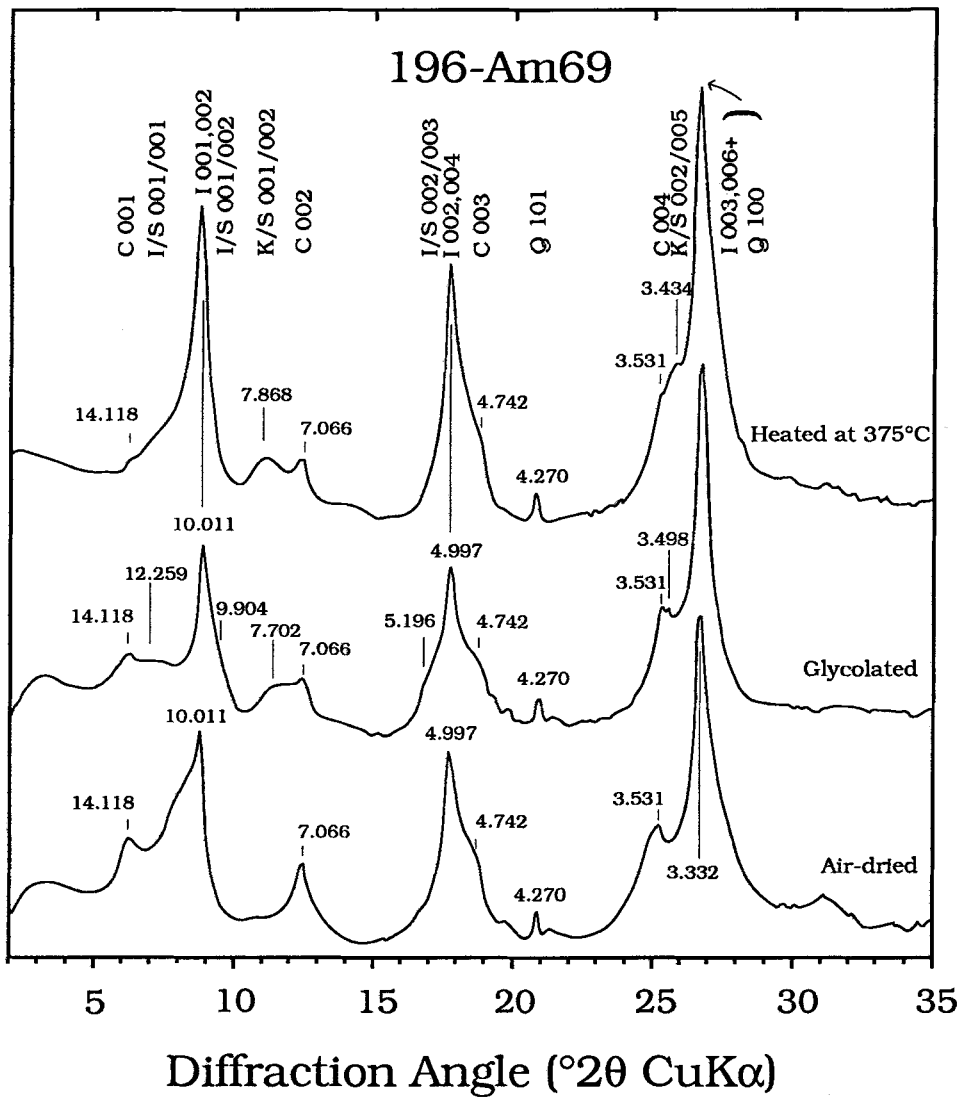

Figure 5. X-ray diffractograms for sample 196-Am69 containing mixed-layer kaolinite/smectite for CuKα radiation.

the transition from the diagenetic zone to the anchizone.

PARAGONITE. (Pg) was identified by its first four basal reflections. However, the first paragonite basal reflection is only barely visible as a weak shoulder on the high-angle side of the first illite basal reflection. The presence of paragonite/muscovite mixed-layer (Pg/Ms) was identified by two reflections at 4.9 and 3.26 Å. 30 occurrences of paragonite, including those of Pg/Ms, from various stratigraphic and tectonic units are depicted in Figure 4, and comparison with Figure 2 shows that paragonite begins to appear from the beginning of the anchizone.

CHLORITOID. (Cld) was reported from a single locality in the study area by Frey and Wieland (1975). This chloritoid was found in middle Jurassic slates belonging to the parautochthonous cover of the Aar massif south of the Vättis window (Figure 6). The growth of chloritoid postdates the main phase of folding and thrusting (Calanda phase) in the Infrahelvetic complex (Pfiffner 1982).

GLAUCONITE. (Glt) was identified under the optical microscope. On XRD traces, glauconite yields a strong first and a very weak second basal reflection and a (060) reflection at 1.51 Å. 30 occurrences of glauconite are indicated in Figure 7, mainly from Cretaceous limestones and sandstones of the Garschella formation ("Gault") of the Säntis nappe. All these occurrences are restricted to the diagenetic zone.

Frey et al. (1973) described the progressive meta-

https://doi.org/10.1346/CCMN.1996.0440109 Published online by Cambridge University Press

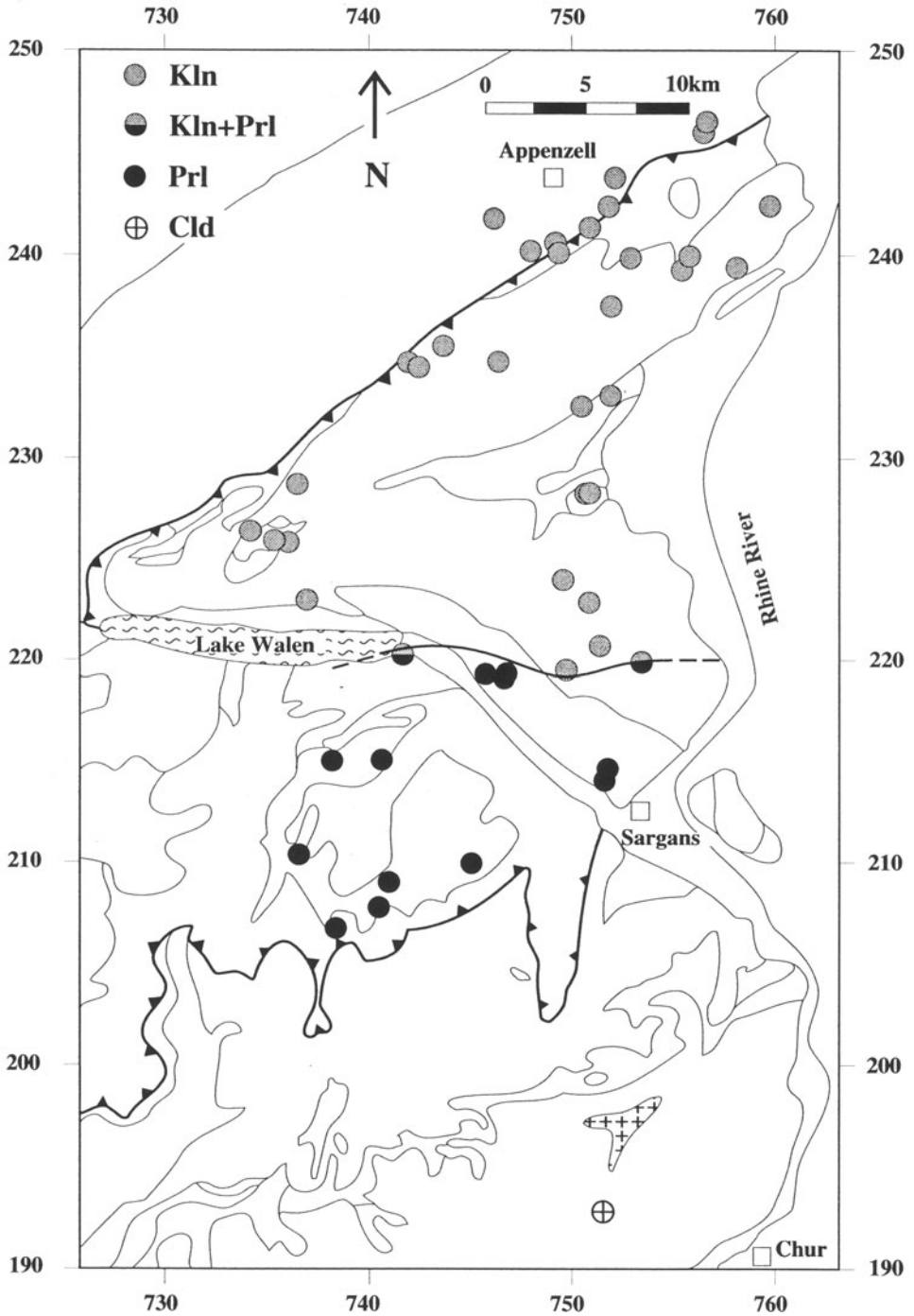

Figure 6. Distribution map for kaolinite, pyrophyllite and chloritoid. The isograd Kln + Qtz = Prl + H_2O crosses tectonic nappe boundaries (cf. Figure 1).

morphism of glauconite-bearing formations and distinguished three metamorphic zones in the Glarus Alps. The new occurrences of glauconite reported in this study (Figure 7) allow one to map the zone I/II boundary in some detail, corresponding to the isograd Glt + Qtz ± Chl = Stp + Kfs + H_2O + O_2. The presence of neoformed K-feldspar as a product was documented by Frey et al. (1973).

STILPNOMELANE. (Stp) occurrences in Figure 7 were already depicted by Frey (1987a, Figure 2.12) but without giving further details. The three occurrences in the

https://doi.org/10.1346/CCMN.1996.0440109 Published online by Cambridge University Press

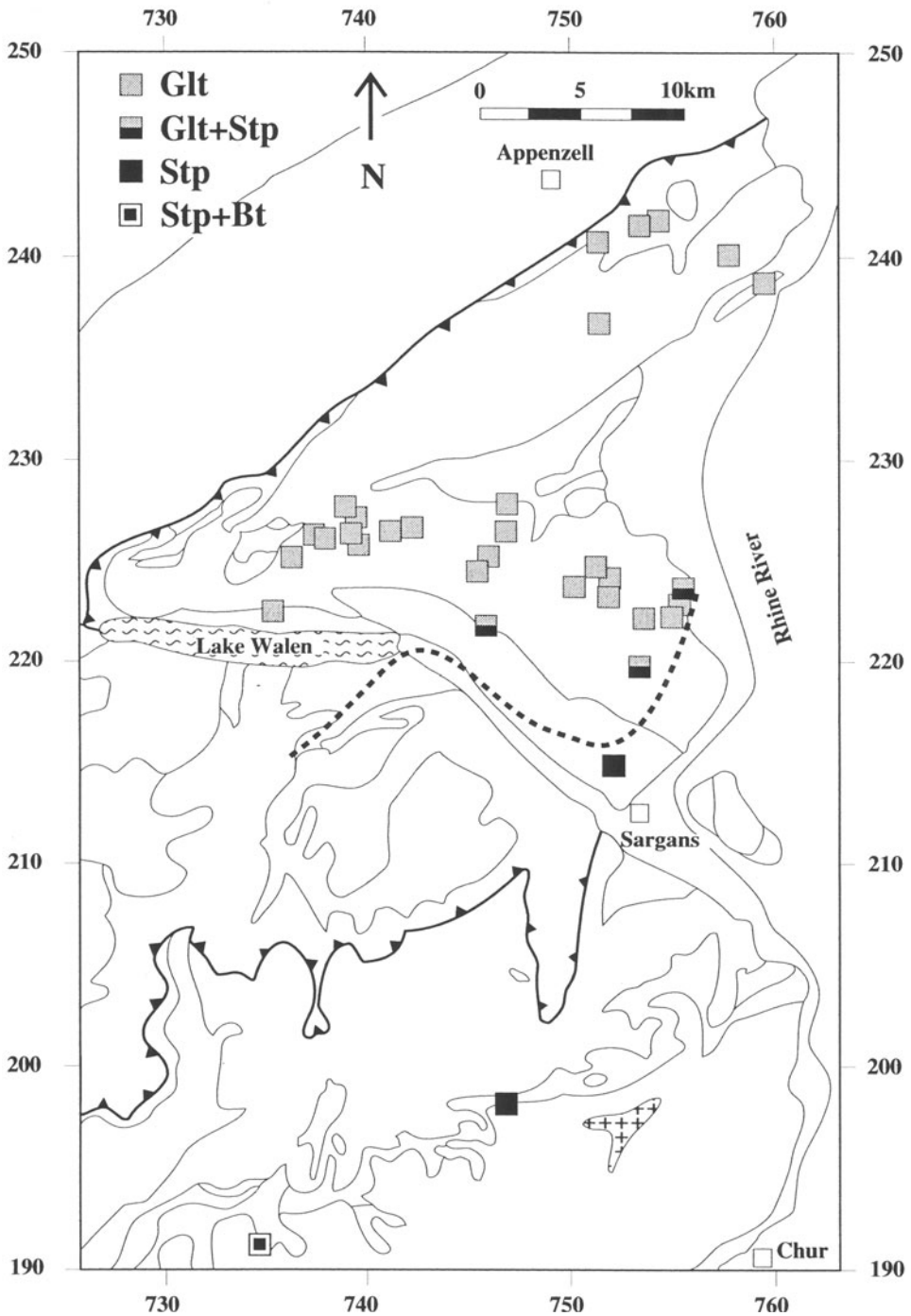

Figure 7. Distribution map for glauconite, stilpnomelane and biotite. The isograd for Glt + Qtz + Chl = Stp + Kfs + fluid is shown as a dashed line parallel to the IC lines of Figure 2.

southern part of the Säntis nappe are from Cretaceous glauconite beds (Altmannschichten and "Gault"). The northernmost of these three localities with coexisting Glt + Stp was first described by Ouwehand (1987, p. 162) from a quarry located SW of Räfis in the Rhine valley. Note that these occurrences of stilpnomelane are located in the diagenetic zone, about 2–3 km downgrade from the beginning of the anchizone, in accordance with observations by Breitschmid (1982) from the Reuss Valley, some 70 km further west-southwest. The stilpnomelane occurrence in the Axen nappe directly north of Sargans is from middle Juras-

https://doi.org/10.1346/CCMN.1996.0440109 Published online by Cambridge University Press

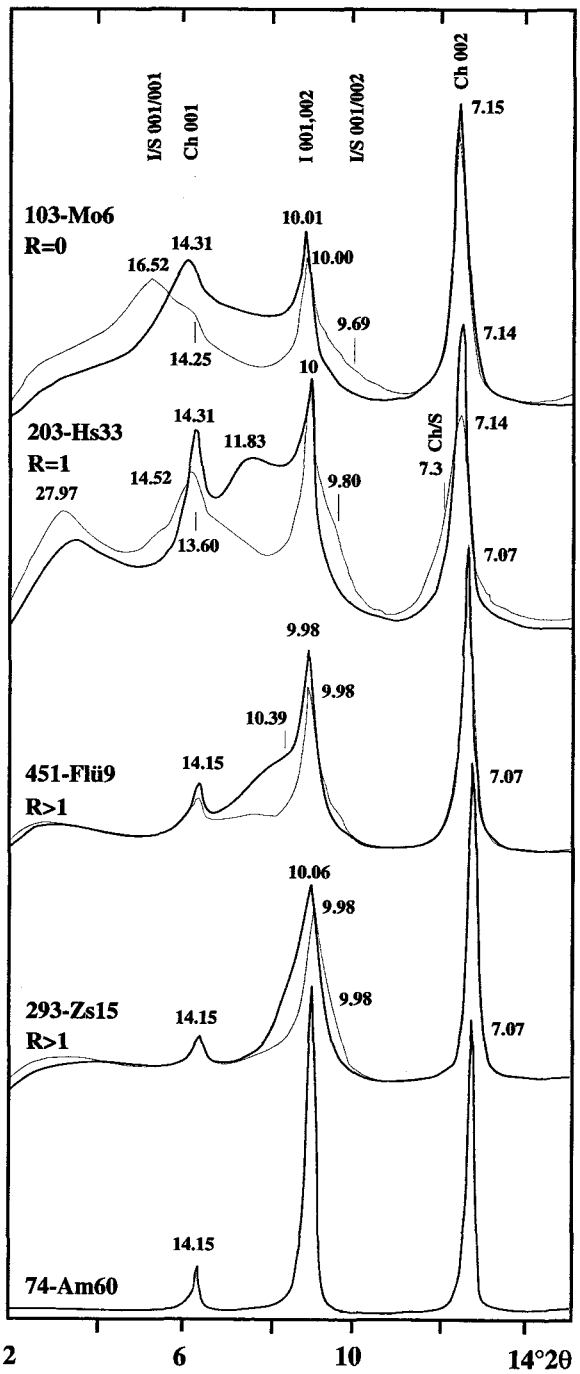

Figure 8. X-ray diffractograms for five representative samples arranged from north (103-Mo6) to south (74-Am60). Thick lines refer to air-dried patterns, thin lines to glycolated patterns. The ordering state R of mixed-layer illite/smectite is indicated. (CuKα radiation).

sic iron ore (Niggli and Niggli 1965). The stilpnomelane locality west of the Vättis window is from the Cretaceous (Lidernenschichten) of the parautochthonous cover of the Aar massif. The occurrence with Stp + Bt at the southern end of the study area was mentioned by Frey et al. (1973, Abb. 3) and is also from the Cretaceous of the parautochthonous cover of the Aar massif. Bürgisser and Felder (1974) have shown that the growth of such epizonal stilpnomelane postdates the main phase of folding and thrusting (Calanda phase) in the Infrahelvetic complex.

Ordering of Illite/Smectite

GENERAL. Ordering of mixed-layer illite/smectite (I/S), interpreted from XRD profiles, correlate with changes in temperature due to burial depth (Pollastro 1993). The alternation and position in d-spacing of I/S basal reflections after glycolation can be used to determine the different ordering types and percentage of illite in I/S (Moore and Reynolds 1989). A reflection at 5 °2Θ indicates random interstratification (Reichweite = R = 0), one near 6.5 °2Θ indicates R1 ordering, and a noticeable peak at angles greater than about 7 °2Θ suggests long-range ordering, that is R > 1 (Moore and Reynolds 1989, p. 252).

RESULTS. The Reichweite (ordering type) and the percentage of illite in I/S were determined using the method of Moore and Reynolds (1989) and the computer program NEWMOD (Reynolds 1985). Representative diffraction patterns arranged according to diagenetic/metamorphic grade are shown in Figure 8, and the calibration curve used to estimate the illite percentage in I/S is depicted in Figure 9.

In our study area I/S is abundant in the diagenetic zone, less abundant in the lower anchizone and not detectable in the higher anchizone and the epizone. The ordering type and the illite content in I/S were determined in 279 samples, and the following four zones are distinguished (Figure 10):

Zone 1 is defined by the presence of randomly interstratified I/S (R = 0) with 20–50% illite in I/S. The ordering types R = 1 with 50–85% illite in I/S and R > 1 with >85% illite in I/S are also found in this zone. Zone 1 is present in the NE part of the study area.

Zone 2 is defined by the presence of the I/S ordering type R = 1 with 50–85% illite in I/S and the absence of the R = 0 type. The ordering type R > 1 with >85% illite in I/S is also found in this zone. Zone 2 covers large parts of the Säntis nappe, including South Helvetic units and Penninic klippes.

Zone 3 is defined by the presence of the I/S ordering type R > 1 with 85–90% illite in I/S and the absence of the R = 1 type. The ordering type R > 1 with >90% illite in I/S is also found in this zone. Zone 3 comprises the SE part of the Säntis nappe, a major

https://doi.org/10.1346/CCMN.1996.0440109 Published online by Cambridge University Press

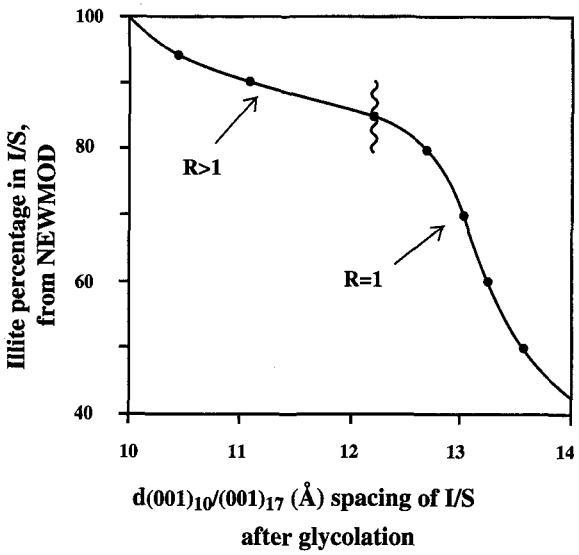

Figure 9. Calibration curve used to estimate the illite percentage in mixed-layer illite/smectite. The curve is valid for "dimica (1 Fe, 0.7 K) mixed with trismectite (1 Fe, 2 gly)" using the terminology of NEWMOD (Reynolds 1985).

part of the Axen nappe northeast of the Seez valley, and the Mürtschen nappe N of Lake Walen.

Zone 4 is defined by the presence of the I/S ordering type R > 1 with >90% illite in I/S and the absence of the other ordering types mentioned above. Zone 4 is mainly found in the Axen nappe N and NW of Sargans, the Fläscherberg, the Mürtschen nappe SE of lake Walen, and in the Infrahelvetic complex S and SE of Sargans.

DISCUSSION. Zones 1–3 mentioned above are covering the diagenetic zone as defined by IC data. In other words, ordering L of I/S is a more sensitive indicator of diagenetic grade than IC.

As recently reviewed by Pollastro (1993), the changes in ordering of I/S may be used as a reliable semiquantitative geothermometer. However, in zones 1–3 described above different ordering types were found, presumably due to lithologic control and the presence of detrital clay minerals. Therefore, this geothermometer cannot be applied in our study area.

Domain Size of Illite in the C-direction

GENERAL. XRD line broadening is caused by the coherent crystalline domain size or crystallite size, lattice strain and instrumental factors (Klug and Alexander 1974, p. 618). The domain size of clay minerals may be used as an indicator of incipient metamorphism (Eberl et al. 1990). At least six methods exist separating the domain size from the general XRD line broadening (Scherrer 1918; Stokes 1948; Warren and Averbach 1950; Ergun 1968; Langford 1978; Balzer and Ledbetter 1993). In the present study, the Warren-Averbach technique is used to measure illite domain size.

RESULTS. Line profiles of the first illite basal reflection obtained after deconvolution were analyzed on air-dried specimens by the Warren-Averbach method for 35 samples. In general, the position of the maximum frequency position increases and domain size distributions spread out as diagenetic/metamorphic grade increases. In the study area, the mean domain size of illite increases from 11 nm in the north to 145 nm in the south, with a major change occurring between km 210 and km 190 of the Swiss coordinate system. With respect to illite "crystallinity," the illite average column length does not change much within the diagenetic zone, but shows a large increase within the anchi- and epizone (Figure 11).

The domain size of illite/smectite was also measured with the Warren-Averbach method, and it was always found to be thinner than that of accompanying illite. I/S domain size increases from 7 nm in the North to 34 nm in the South, therefore showing the same general tendency as illite.

DISCUSSION. Assuming the presence of strain-free illite, the Scherrer equation was also used to calculate the mean domain size of illite. A range from 7 to 97 nm was obtained, compared with 11–145 nm by the Warren-Averbach method. This difference may be explained by the fact that the Scherrer equation does not take account of the strain effects. Furthermore, the Warren-Averbach technique is model-dependent and will not correspond to a real distribution of grain sizes of natural clays that may preserve strain across semicoherent packets, as discussed by Lanson and Kübler (1994).

Eberl et al. (1990) analyzed the particle thickness distributions for 20 anchizonal and epizonal illites from shales from the Glarus Alps, located directly in the West of our study area. The general shape of particle thickness distribution curves obtained was similar to those derived in this study, and it was concluded that these illites underwent recrystallization by Ostwald ripening. However, these authors reported smaller illite average column length values than obtained for illites of comparable grade in this study; e.g., <35 nm (Eberl et al. 1990) vs 100–145 nm (this study) for epizonal illites. More work is needed to explain this discrepancy.

Most recently, Warr and Rice (1994) proposed illite domain (crystallite) sizes of 23 for the lower and 52 nm for the upper limit of the anchizone determined by the Warren-Averbach method. These values are much smaller than the limiting values of about 50 and 100 nm determined in this study. It should be mentioned that Warr and Rice (1994) were using glycolated specimens for the domain size analyses but made a correlation with illite "crystallinity" determined on air-

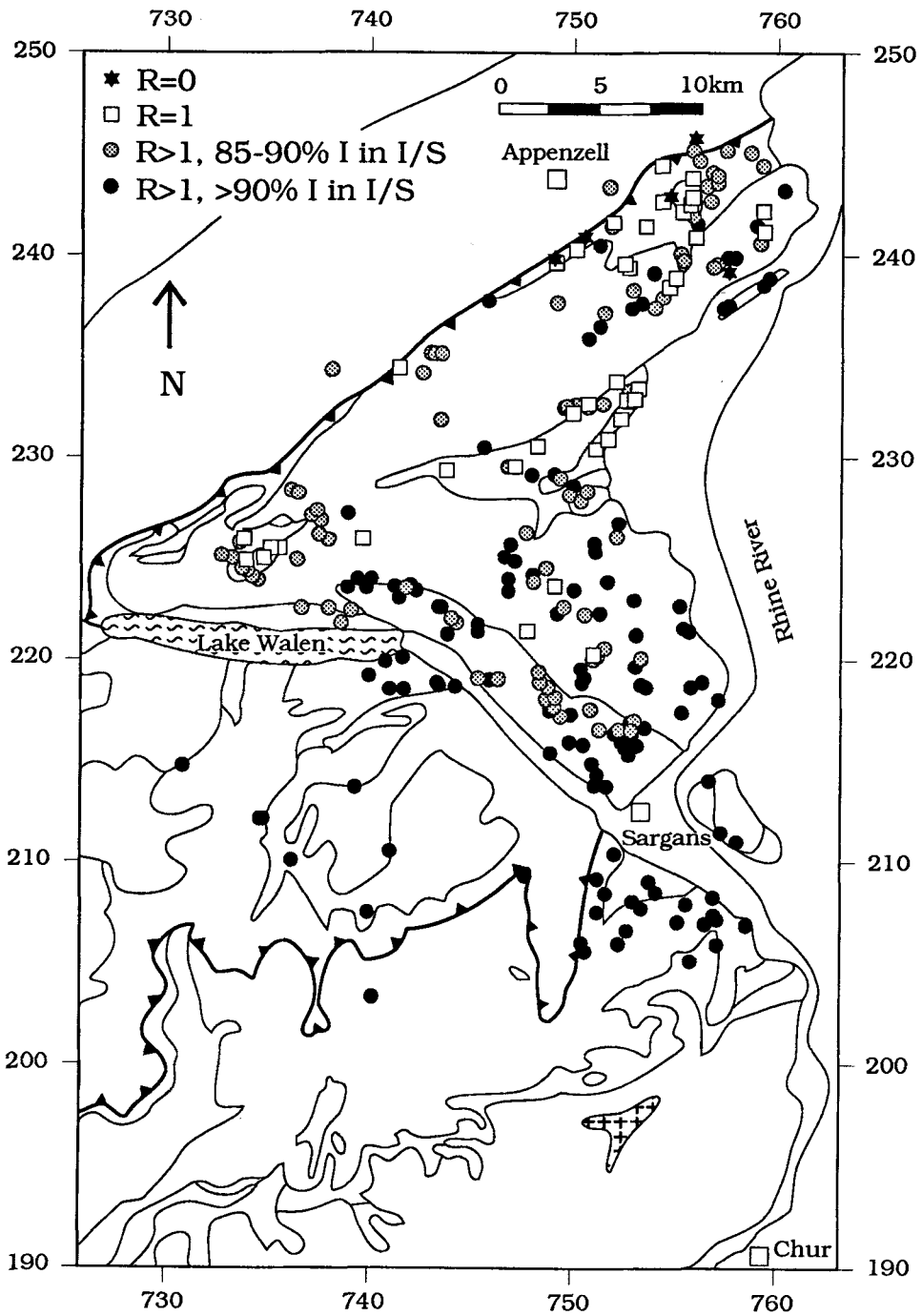

Figure 10. Distribution map for different ordering types of mixed-layer illite/smectite and percentage of illite in I/S. These data allow for a four-fold zonation as discussed in text.

dried specimens. In addition, the correlation proposed by these authors is based on four specimens only. The authors of this article feel that much more experience is needed with domain size analyses and that the limiting values of Warr and Rice (1994) should be regarded with caution.

Chlorite Polytypes

GENERAL. During late diagenesis and incipient metamorphism a change in the polytype of trioctahedral chlorite is observed. Hayes (1970) proposed that the polytype transformation sequence $Ib_d \rightarrow Ib$ ($\beta = 97°$)

https://doi.org/10.1346/CCMN.1996.0440109 Published online by Cambridge University Press

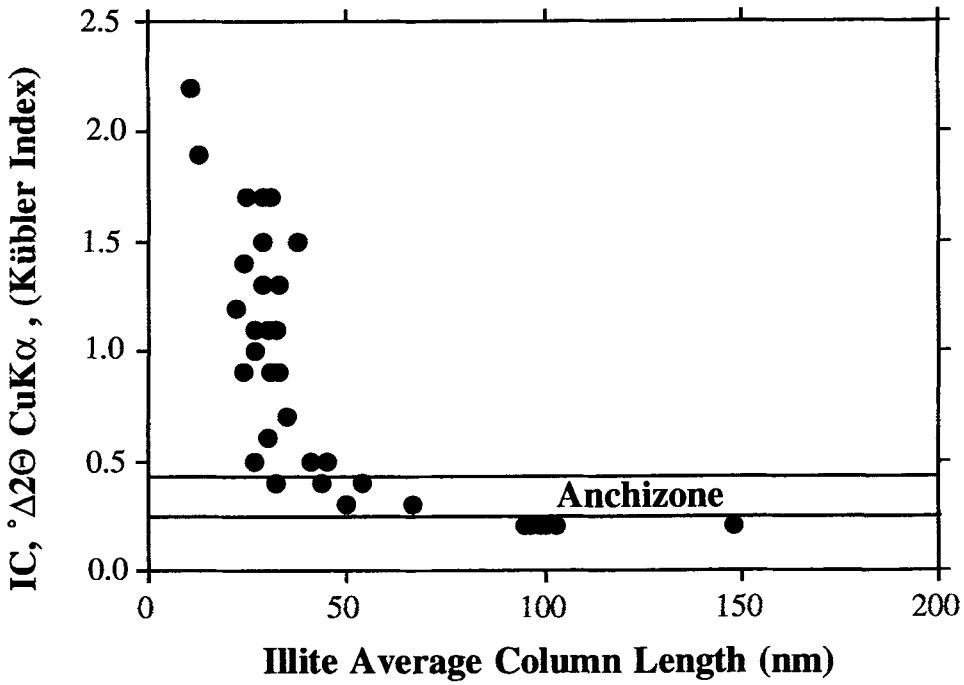

Figure 11. Variation of illite domain size or illite average column length vs illite "crystallinity" (Kübler index).

→ I*b* (β = 90°) → II*b* (β = 97°) occurs in chlorites in sedimentary rocks with increasing temperature, and that the final transformation from type-I to type-II chlorite requires a temperature of about 150–200°C. However, as recently reviewed by Walker (1993), other factors including grain size of the host rock, may be at least as important as temperature in controlling the stability of type-I chlorite polytypes. In addition, systematic studies suggest that type-II chlorite is stable at temperatures well below 200°C and that it can form as the initial chlorite phase without passing through any intermediate polytypic stages (Walker 1993).

RESULTS. Chlorite polytypes were determined on 19 chlorite-rich samples following the methods proposed by Bailey (1988) and Moore and Reynolds (1989). Interference with illite reflections were stripped by using deconvolution technique. For 12 samples from the diagenetic zone (5 sandstones, 4 pelites and 3 limestones), exclusively the I*b* (β = 90°) polytype was found, while in 7 pelites and marls from the anchizone and epizone only the IIb chlorite polytype was present.

DISCUSSION. If compared to other indicators of incipient metamorphism in the study area, the simple chlorite polytype distribution pattern seems to follow the observations made by Hayes (1970), for example the I*b* (β = 90°) chlorite polytype of the diagenetic zone is followed by the IIb polytype in the anchizone and epizone. Therefore, the chlorite polytype conversion in the study area appears to be controlled mainly by temperature.

b_o of illite

GENERAL. The b_o cell parameter of muscovite or illite may be used as a semiquantitative geobarometer for epizonal (Sassi and Scolari 1974) or upper anchizonal (Padan et al. 1982) shales and slates. This geobarometer is based on two observations: 1) the celadonite content of potassic white mica increases with increasing pressure (if temperature is held constant); and 2) there exists a positive correlation between the b_o parameter and celadonite content. Although this barometer uses unbuffered assemblages lacking K-feldspar, it has been successfully applied in many field areas. Therefore, the statement by Essene (1989) that "it seems prudent to avoid the use of Sassi's phengite barometer for thermobarometry" seems not justified.

RESULTS. The b_o parameter is usually determined through the measurement of the d(060) spacing. If randomly oriented preparates are used for that purpose, as was attempted in this study, then the (060) peak is overlapped and obscured by the ($\bar{3}31$) peak and additional weak reflections. In order to test the reliability of our b_o determinations through the measurement of illite d(060, $\bar{3}31$) values, the b_o cell dimension was also calculated from a unit cell refinement using at least 20 reflections. Results of this comparison for 33 samples ranging in grade from the diagenetic zone to the epizone show a rather good linear correlation (Figure 12). b_o values calculated from d(060, $\bar{3}31$) are slightly smaller than b_o values obtained from unit cell refinement, with a maximum deviation of 0.015 Å.

https://doi.org/10.1346/CCMN.1996.0440109 Published online by Cambridge University Press

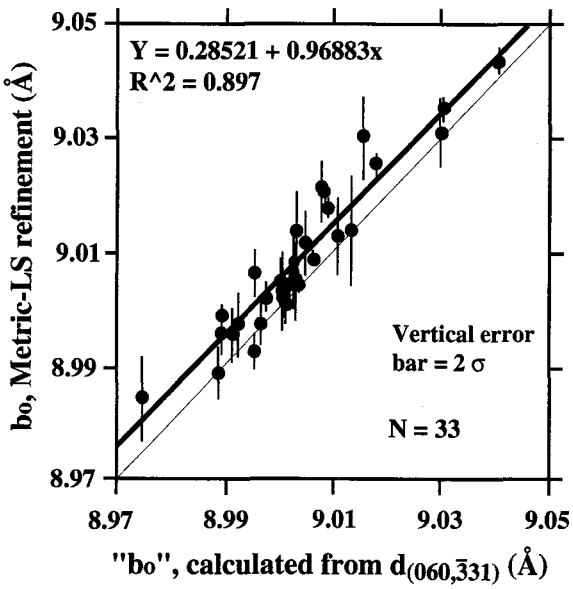

Figure 12. b_o values calculated from d($\bar{3}$31, 060) vs b_o values calculated after least-square refinement. The thick line refers to correlated data, the thin line is the equal data line.

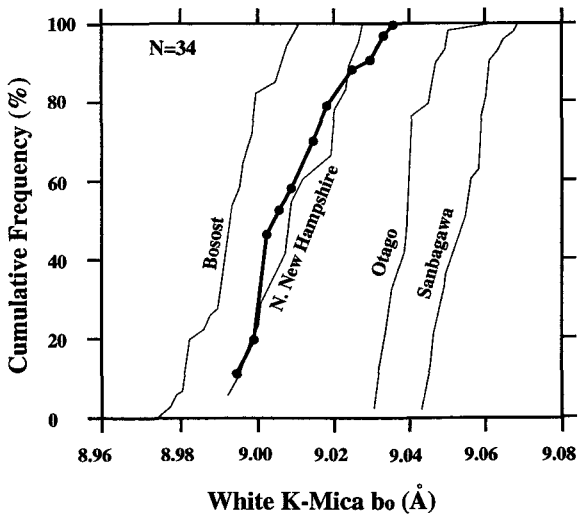

Figure 13. Cumulative frequency curve of illite b_o values for 34 anchizonal and epizonal samples (thick line). Reference curves (thin lines) are from Sassi and Scolari (1974).

This result is to be expected because the ($\bar{3}$31) peak has a smaller d-value than the (060) peak (e.g., Borg and Smith 1969). In conclusion, for illite b_o-geobarometry using randomly oriented preparates, the b_o parameter may be calculated from the relation $b_o = 6 \times$ d(060, $\bar{3}$31) with some confidence.

The d(060, $\bar{3}$31) values for 32 illites (including illite/smectite mixed-layer) from the Säntis nappe range from 1.495–1.503 Å (mean value 1.499 Å), for 12 lower anchizonal illites range from 1.500–1.506 Å (mean value 1.502 Å), and for 18 upper anchizonal and 4 epizonal illites range from 1.499–1.506 Å (mean value 1.501 Å).

DISCUSSION. b_o or d(060, $\bar{3}$31) of illite increases in the study area with grade during incipient metamorphism, in accordance with results reported by Padan et al. (1982) and Yang and Hesse (1991). The b_o parameter increases with an increasing replacement of Al by Fe + Mg in the octahedral layer and K in the interlayer position (Radoslovich and Norrish 1962; Hunziker et al. 1986). The general decrease of expandable layers in illite/smectite from north to south means a concomitant increase of K, but whether Fe + Mg are also increasing is not known.

Because lower and upper anchizonal illites of the study area yielded almost identical b_o values, lower anchizonal samples were included in b_o geobarometry. A cumulative frequency plot of b_o values for anchi- and epimetamorphic samples indicates conditions of an intermediate-pressure facies series as for northern New Hampshire (Figure 13). The mean b_o value of 9.010 Å obtained for the southern part of the study area is very similar to the 9.013 Å reported by Frey (1988) for North Helvetic flysch from the adjacent Glarus Alps.

Correlation Between Indicators of Incipient Metamorphism

The mineral distribution with increasing grade is summarized in Figure 14. The presence of smectite in the Subalpine Molasse at vitrinite reflectance <0.6% Rmax (Erdelbrock 1994) indicates diagenetic zone 2 of Kübler et al. (1979). Kaolinite is a typical index mineral of the diagenetic zone, and the isograd Kln +

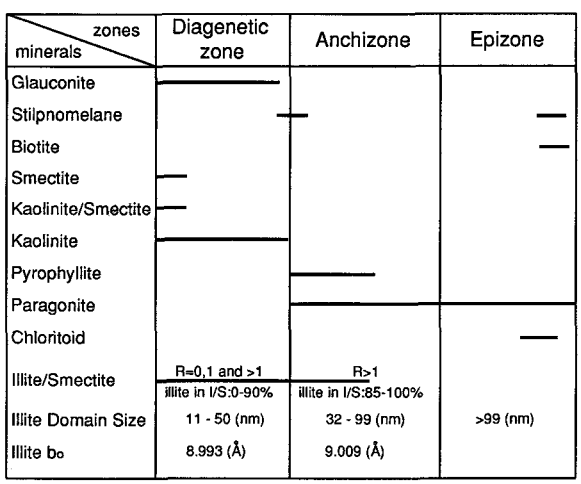

Figure 14. Summary of indicators of diagenesis and incipient metamorphism for the Helvetic Alps of eastern Switzerland. The distribution of index minerals and various properties of mixed-layer illite/smectite and illite are plotted against grade as defined by illite "crystallinity" data.

https://doi.org/10.1346/CCMN.1996.0440109 Published online by Cambridge University Press

Qtz = Prl + H_2O is located at the beginning of the anchizone (Figures 2 and 6). Physical conditions for two localities along this isograd (Figure 6, stations with Kln + Prl) were estimated as 240–260°C/2.1 kbar based on coal rank and fluid inclusion data (Frey 1987b). Paragonite is widespread in the anchizone and epizone. Glauconite-bearing sandstones and limestones are widespread in the diagenetic zone, and the isograd Glt + Qtz ± Chl = Stp + Kfs + fluid is located in the uppermost diagenetic zone.

Several properties of mixed-layer illite/smectite and illite are also useful indicators of incipient metamorphism. The ordering type or Reichweite of I/S changes from R = 0 to R > 1, although different ordering types were found within a restricted area. Nevertheless this allowed to distinguish four zones with different R values and illite contents in I/S, and three of these zones allowed a subdivision of the diagenetic zone as defined by illite "crystallinity." Illite domain size generally increases with increasing grade, and limiting values of 50 and 100 nm were determined for the lower and upper boundaries of the anchizone.

Regional Significance

Three main tectonic features of the study area are the Glarus thrust, the Säntis thrust and the basal Penninic thrust. In this section, possible breaks in diagenetic or metamorphic grade across these thrusts will be discussed.

The presence of dioctahedral smectite in the Subalpine Molasse and its absence in similar lithologies of the Säntis nappe indicates a higher diagenetic grade for the upper tectonic unit (Figure 1). Such a break in grade was also observed by Erdelbrock (1994) based on vitrinite reflectance data: Rmax < 0.6% for the Subalpine Molasse around Appenzell and Rmax > 1.3% for the adjacent Säntis nappe. Using the terminology of Kübler et al. (1979), the Subalpine Molasse belongs to the diagenetic zone 2 whereas the Säntis nappe belongs to zones 3 and 4. Obviously, the higher grade Säntis nappe dislocated along the Glarus thrust over the Subalpine Molasse causing a discontinuous inverse diagenetic zonation.

The Helvetic nappes show a general increase in diagenetic/metamorphic grade from north to south, mainly documented by the regional distribution of various index minerals, illite "crystallinity" data, the overall diminution of expandable layers and the ordering of illite/smectite. Within the Helvetic nappe pile, grade increases from tectonically higher to lower units. This is best documented in the Alvier-Sargans-lake Walen area by vitrinite reflectance data (Erdelbrock 1994), but is also supported by IC data (Figure 2) and the Kln → Prl conversion (Figure 6). As mentioned earlier, the diagenesis/anchizone boundary as well as the isograds Kln + Qtz = Prl + H_2O and Glt + Qtz ± Chl = Stp + Kfs + fluid almost coincide in the study area, and are crossing nappe boundaries, including the Säntis thrust, thus indicating that incipient metamorphism was a late syn- to post-nappe-forming event.

Further to the south, in the Pizol area, IC data indicates a discontinuous inverse metamorphic zonation across the Glarus thrust, separating the Verrucano from the Infrahelvetic complex, with some 5–10 km of post-metamorphic thrusting. This feature is in accordance with the discontinuous inverse diagenetic zonation near the Alpine border mentioned above.

Available data from this study and Erdelbrock (1994) show no difference in diagenetic grade between the Säntis nappe and Penninic klippen, indicating no break in diagenetic grade across the basal Penninic thrust, and thus a common late diagenetic history for these tectonic units.

ACKNOWLEDGMENTS

Most samples used in this study were collected by Kersten Erdelbrock. The first author is grateful to Josef Mullis for his help during field investigations and additional sample collections. Reynald Handschin guided with the preparation of randomly oriented sample. Michael Dalla Torre and Meinert Rahn provided additional help. Dennis D. Eberl and Eric Essene kindly reviewed the manuscript and improved the English. The first author was supported by Basel University.

REFERENCES

Árkai P. 1991. Chlorite crystallinity: an empirical approach and correlation with illite crystallinity, coal rank and mineral facies as examplified by Palaeozoic and Mesozoic rocks of northeast Hungary. J Metamorph Geol 9:723–734.

Bailey SW. 1988. X-ray diffraction identification of the polytypes of mica, serpentine, and chlorite. Clays & Clay Miner 36:193–213.

Balzer D, Ledbetter H. 1993. Voigt-function modeling in Fourier analysis of size- and strain-broadened X-ray diffraction peaks. J Appl Cryst 26:97–103.

Borg IY, Smith DK. 1969. Calculated X-ray powder patterns for silicate minerals. Mem Geol Soc Am 122:896 p.

Breitschmid A. 1982. Diagenese und schwache Metamorphose in den sedimentären Abfolgen der Zentralschweizer Alpen. Eclogae Geol Helv 75:331–380.

Briegel U. 1972. Geologie der östlichen Alviergruppe, unter besonderer Berücksichtigung der Drusberg-und Schrattenkalkformation. Eclogae Geol Helv 65:425–483.

Burger H. 1982. Tonmineralogische und sedimentpetrographische Untersuchungen in der untersten Kreide des östlichen Helvetikums. Schweiz Mineral Petrogr Mitt 62: 369–414.

Bürgisser HM, Felder TE. 1974. Zur Geologie der Südabdachung der Segnas-Ringel-Gruppe (Vorderrheintal, Graubünden). Eclogae Geol Helv 67:457–467.

Eberl DD, Srodon J, Kralik M, Taylor BE, Peterman ZE. 1990. Ostwald ripening of clays and metamorphic minerals. Science 248:474–477.

Erdelbrock K. 1994. Diagenese und schwache Metamorphose im Helvetikum der Ostschweiz (Inkohlung und Illit-"Kristallinität"). Diss Rhein-Westf Techn Hochschule Aachen 219 S.

Erdelbrock K, Wolf M, Krumm H, Frey M. 1993. Vitrinite reflectance data from a transect through the Helvetic Zone of eastern Switzerland. TERRA abstracts, Suppl. No 1 to TERRA nova 5:415.

Ergun S. 1968. Direct method for unfolding convolution

products—its application to X-ray scattering intensities. J Appl Cryst 1:19–23.
Essene EJ. 1989. The current status of thermobarometry in metamorphic rocks. In:Daly JS, Cliff RA, Yardley BWD, editors. Evolution of Metamorphic Belts. Geol. Soc. Spec. Pub. London:Geol Soc 43:1–44.
Frey M. 1970. The step from diagenesis to metamorphism in pelitic rocks during Alpine orogenesis. Sedimentol 15: 261–279.
Frey M. 1986. Very low-grade metamorphism of the Alps—an introduction. Schweiz Mineral Petro Mitt 66:13–27.
Frey M. 1987a. Very low-grade metamorphism of clastic sedimentary rocks. In:Frey M, editor. Low Temperature Metamorphism. Glasgow: Blackie. 9–58.
Frey M. 1987b. The reaction-isograd kaolinite + quartz = pyrophyllite + H_2O, Helvetic Alps, Switzerland. Schweiz Mineral Petro Mitt 67:1–11.
Frey M. 1988. Discontinuous inverse metamorphic zonation, Glarus Alps, Switzerland: evidence from illite "crystallinity" data. Schweiz Mineral Petro Mitt 68:171–183.
Frey M, Hunziker JC, Roggwiller P, Schindler C. 1973. Progressive niedriggradige Metamorphose glaukonitführender Horizonte in den helvetischen Alpen der Ostschweiz. Contrib Mineral Petrol 39:185–218.
Frey M, Wieland B. 1975. Chloritoid in autochthonparautochthonen Sedimenten des Aarmassivs. Schweiz Mineral Petro Mitt 55:407–418.
Handschin R, Stern WB. 1989. Preparation and analysis of microsamples for X-ray diffraction and -fluorescence. SIEMENS Anal Appl Note 319.
Hayes JB. 1970. Polytypism of chlorite in sedimentary rocks. Clays & Clay Miner 18:285–306.
Hunziker JC, Frey M, Clauer N, Dallmeyer RD, Friedrichsen H, Flehmig W, Hochstrasser K, Roggwiller P, Schwander H. 1986. The evolution of illite to muscovite: mineralogical and isotopic data from the Glarus Alps, Switzerland. Contrib Mineral Petrol 92:157–180.
Klug HP, Alexander LE. 1974. X-Ray Diffraction Procedures, 2nd ed. New York:Wiley. 966p.
Kübler B. 1967. La cristallinité de l'illite et les zones tout à fait supérieures du métamorphisme. Etages tectoniques, Colloque à Neuchâtel 1966. Neuchâtel, Suisse:A la Baconnière. 105–121.
Kübler B. 1968. Evaluation quantitative du métamorphisme par la cristallinité de l'illite. Bull Cent Rech Pau-SNPA 2: 385–397.
Kübler B, Pitton J-L, Héroux Y, Charollais J, Weidmann M. 1979. Sur le pouvoir réflecteur de la vitrinite dans quelques roches du Jura, de la Molasse et des nappes préalpines, helvétiques et penniques. Eclogae Geol Helv 72:347–373.
Langford JI. 1978. A rapid method for analysing the breadths of diffraction and spectral lines using the Voigt function. J Appl Cryst 11:10–14.
Lanson B, Kübler B. 1994. Experimental determinations of the coherent scattering domain size distribution of natural mica-like phases with the Warren-Averbach technique. Clays & Clay Minerals 42:489–494.
Moore DM, Reynolds RC. 1989. X-Ray Diffraction and the Identification and Analysis of Clay Minerals. Oxford, New York:Oxford University Press. 332p.
Niggli E, Niggli CR. 1965. Karten der Verbreitung einiger Mineralien der alpidischen Metamorphose in den Schweizer Alpen (Stilpnomelan, Alkali-Amphibol, Chloritoid, Staurolith, Disthen, Sillimanit). Eclogae Geol Helv 58:335–368.
Ouwehand P. 1987. Die Garschella-Formation ("Helvetischer Gault", Aptian-Cenomanian) der Churfirsten-Alvier Region (Ostschweiz), Sedimentologie, Phosphoritgenese, Stratigraphie. Mitt Geol Inst ETH u Univ Zürich NF 275.
Padan A, Kisch HJ, Shagam R. 1982. Use of the lattice parameter bo of dioctahedral illite/muscovite for the characterization of P/T gradients of incipient metamorphism. Contrib Mineral Petrol 79:85–95.
Pfiffner OA. 1986. Evolution of the north Alpine foreland basin in the Central Alps. Spec Publ Int Assoc Sedimentol 8:219–228.
Pfiffner OA. 1982. Deformation mechanisms and flow regimes in limestones from the Helvetic zone of the Swiss Alps. J Struct Geol 4:429–442.
Pfiffner OA, Frei W, Valasek P, Stäuble M, Levato L, DuBois L, Schmid SM, Smithson SB. 1990. Crustal shortening in the Alpine Orogen: results from deep seismic reflection profiling in the eastern Swiss Alps, line NFP 20-east. Tectonics 9:1327–1355.
Pollastro RM. 1993. Considerations and applications of the illite/smectite geothermometer in hydrocarbon-bearing rocks of Miocene to Mississippian age. Clays & Clay Miner 41:119–133.
Radoslovich EW, Norrish K. 1962. The cell dimensions and symmetry of layer-lattice silicates: I. Some structural consideration. Amer Mineral 47:599–617.
Reynolds RC. 1985. NEWMOD, a computer program for the calculation of one-dimensional diffraction patterns of mixed-layer clays. Hanover, N.H.:R. C. Reynolds, 8 Brook Rd.
Sassi FP, Scolari A. 1974. The bo value of the potassium white micas as a barometric indicator in low-grade metamorphism of pelitic schists. Contrib Mineral Petrol 45:143–152.
Scherrer P. 1918. Bestimmung der Grösse und der inneren Struktur von Kolloidteilchen mittels Röntgenstrahlen. Göttinger Nachr Math Phys 2:98–100.
Spicher A. 1980. Tektonische Karte der Schweiz. Schweiz geol komm 1:500 000.
Stern WB. 1991. Preparation and cell refinement of mica microsamples. Schweiz Mineral Petro Mitt 71:151–159.
Stokes AR. 1948. A numerical Fourier-analysis method for the correction of width and shapes of lines on X-ray powder photographs. Proc Phys Soc 61:382–391.
Trümpy R. 1980. Geology of Switzerland, Part A. Basel, New York:Wepf & Co. Publishers. 104p.
Velde B. 1985. Clay minerals, a physico-chemical explanation of their occurrence. Dev. Sedimentol. Elsevier, Amsterdam-Oxford-New York-Tokyo 40:427p.
Walker JR. 1993. Chlorite polytype geothermometry. Clays & Clay Miner 41:260–267.
Warr LN, Rice AHN. 1994. Interlaboratory standardization and calibration of clay mineral crystallinity and crystallite size data. J Metamorph Geol 12:141–152.
Warren BE, Averbach BL. 1950. The effect of cold-work distortion on X-ray patterns. J Appl Phys 21:595–599.
Yang C, Hesse R. 1991. Clay minerals as indicators of diagenetic and anchimetamorphic grade in an overthrust belt, external domain of southern Canadian Appalachians. Clay Miner 26:211–231.

(Received 15 November 1994; accepted 12 June 1995; Ms. 2594)